Author(s): Shi, Yue; Dobaczewski, Jacek; Greenlees, Paul

Title: Rotational properties of nuclei around 254 No investigated using a spectroscopic-quality Skyrme energy density functional

Year: 2014

Version:

Please cite the original version:

Shi, Y., Dobaczewski, J., & Greenlees, P. (2014). Rotational properties of nuclei around 254 No investigated using a spectroscopic-quality Skyrme energy density functional. Physical Review C, 89(3), Article 034309. https://doi.org/10.1103/PhysRevC.89.034309

Rotational properties of nuclei around ^{254}No investigated using a spectroscopic-quality Skyrme energy density functional

Yue Shi (石跃),[1,2,3,4] J. Dobaczewski,[3,5] and P. T. Greenlees[3]

[1]*Department of Physics and Astronomy, University of Tennessee, Knoxville, Tennessee 37996, USA*
[2]*Joint Institute for Heavy Ion Research, Oak Ridge National Laboratory, Oak Ridge, Tennessee 37831, USA*
[3]*Department of Physics, P.O. Box 35 (YFL), University of Jyväskylä, FI-40014 Jyväskylä, Finland*
[4]*State Key Laboratory of Nuclear Physics and Technology, School of Physics, Peking University, Beijing 100871, China*
[5]*Institute of Theoretical Physics, Faculty of Physics, University of Warsaw, ul. Hoża 69, PL-00681 Warsaw, Poland*

(Received 16 December 2013; revised manuscript received 22 February 2014; published 17 March 2014)

Background: Nuclei in the $Z \approx 100$ mass region represent the heaviest systems where detailed spectroscopic information is experimentally available. Although microscopic-macroscopic and self-consistent models have achieved great success in describing the data in this mass region, a fully satisfying precise theoretical description is still missing.

Purpose: By using fine-tuned parametrizations of the energy density functionals, the present work aims at an improved description of the single-particle properties and rotational bands in the nobelium region. Such locally optimized parametrizations may have better properties when extrapolating towards the superheavy region.

Methods: Skyrme Hartree-Fock-Bogolyubov and Lipkin-Nogami methods were used to calculate the quasiparticle energies and rotational bands of nuclei in the nobelium region. Starting from the most recent Skyrme parametrization, UNEDF1, the spin-orbit coupling constants and pairing strengths have been tuned, so as to achieve a better agreement with the excitation spectra and odd-even mass differences in ^{251}Cf and ^{249}Bk.

Results: The quasiparticle properties of ^{251}Cf and ^{249}Bk were very well reproduced. At the same time, crucial deformed neutron and proton shell gaps open up at $N = 152$ and $Z = 100$, respectively. Rotational bands in Fm, No, and Rf isotopes, where experimental data are available, were also fairly well described. To help future improvements towards a more precise description, small deficiencies of the approach were carefully identified.

Conclusions: In the $Z \approx 100$ mass region, larger spin-orbit strengths than those from global adjustments lead to improved agreement with data. Puzzling effects of particle-number restoration on the calculated moment of inertia, at odds with the experimental behavior, require further scrutiny.

DOI: 10.1103/PhysRevC.89.034309 PACS number(s): 21.60.Jz, 21.10.Re, 21.10.Pc, 27.90.+b

I. INTRODUCTION

The stability of superheavy elements (SHE) with atomic numbers $Z \geqslant 104$ is entirely due to quantum shell effects. Without such shell effects, strong Coulomb repulsion between the protons would lead to immediate spontaneous fission. Therefore, one of the most important subjects in the study of SHE is nuclear shell structure. However, due to low population cross sections, experimental information on SHE is generally limited to half-lives and α-decay energies, which can only be indirectly related to the shell structure. Only very recently were electromagnetic transitions observed for the first time in the decay chain of ^{288}115 [1]. After decades of experimental studies, the heaviest SHE so far produced has proton number $Z = 118$ [2–4].

Nuclei in the nobelium ($Z = 102$) region are unique in the sense that they are the heaviest systems where detailed spectroscopic information is available [5]. With numerous rotational bands observed [6], the ground states of these nuclei are known to be well deformed, with prolate $\beta_2 \approx 0.3$ shapes. Although the SHE in the elusive superheavy island of stability are thought to be spherical, it can be expected that a proper description of the single-particle (s.p.) structures in the nobelium region would result in a better extrapolation of the shell structure towards the superheavy region.

Theoretical calculations in the nobelium region have been limited to various mean-field models, which can be divided into two large categories: those based on the microscopic-macroscopic model [7–12], and those using self-consistent approaches [13]. The latter used non-relativistic zero-range Skyrme [14–17] or finite-range Gogny [18–20] forces as well as relativistic Lagrangians [21–25]. All these calculations reproduce reasonably well the gross features of experimental rotational spectra, however, differences can be found on detailed inspection.

Experimental quasiparticle energies of odd-A systems in the nobelium region show better agreement with the microscopic-macroscopic calculations [10], which have deformed shell gaps open at $N = 152$ and $Z = 100$. None of the self-consistent approaches, whether in the non-relativistic or relativistic variant, predict such deformed shell gaps for both protons and neutrons; a few of them predict the $N = 152$ or $Z = 100$ shell openings, but not both [26].

The fine details of the shell structure depend on small changes of the model parameters. Up to now, the parameters have been mostly determined by global adjustments to various experimental data across the nuclear chart. It is extremely gratifying to see that these adjustments of a few parameters give a fair overall agreement with a large body of data. However, through these adjustments, a precise description of particular experimental features in a given region of nuclei, such as the transuranium elements, has not been obtained.

The most advanced adjustments of parameters with full error analyses have been performed for the Skyrme energy-density functionals (EDFs) [27–29]. It is by now quite clear that within a limited parametrization of this force, further improvements towards globally precise results are not possible [30,31]. Much less work in this direction has been done for the relativistic approaches and almost none for the Gogny interaction and microscopic-macroscopic models, however, one can reasonably expect that similar conclusions may hold there too.

Various strategies of extending simple parametrizations are now being investigated. However, before these become available and eventually achieve a higher level of precision, one has to look into the possibility of local adjustment of parameters. This is the strategy adopted in the present work. In doing so, the idea of Ref. [32] is followed, where so-called spectroscopic-quality parametrizations, which focus on adjusting the shell-structure properties of nuclei, were proposed.

The paper is organized as follows. In Sec. II the parameters of the model are defined and various adjustments of parameters are discussed. In Sec. III the results obtained are presented and analyzed. Finally, in Sec. IV the conclusions that can be drawn from the study are presented.

II. THE MODEL

In this study, calculations were performed using the symmetry-unrestricted solver HFODD (v2.52j) [33,34]. The Skyrme Hartree-Fock-Bogolyubov (SHFB) equations were solved by expanding the mean-field wave functions on 680 deformed harmonic-oscillator (HO) basis states, with HO frequencies of $\hbar\Omega_x = \hbar\Omega_y = 8.4826549$ MeV and $\hbar\Omega_z = 6.4653456$ MeV. This corresponds to including the HO basis states up to $N_x = N_y = 13$ and $N_z = 14$ quanta. To study any possible impact of the finite HO space, calculations were also performed using a larger basis of 969 states and $N_x = N_y = 15$ and $N_z = 19$ quanta.

In odd-mass nuclei, quasiparticle excitations are obtained by blocking the relevant levels when performing the SHFB calculations. The procedure closely follows that of Ref. [35]. The excitation spectra are obtained by taking differences of the total energies obtained by blocking different orbitals.

The recently proposed Skyrme parametrization UNEDF1 [29] was used, for which local adjustments of the spin-orbit (SO) strength were performed, while keeping all other parameters unchanged (see below). The parameter set obtained is denoted by UNEDF1$^{\rm SO}$. For comparison, the results obtained using an older standard Skyrme parametrization SLy4 [36] were calculated. The final calculations were performed for the force UNEDF1$^{\rm SO}_{\rm L}$, for which the time-odd coupling constants were determined by the Landau parameters and local-gauge-invariance arguments, as defined in Ref. [37].

In the pairing channel, the mixed pairing force [38] was adopted, both with and without Lipkin-Nogami (LN) approximate particle-number projection [39]. These two variants of the calculation are denoted by SHFB+LN and SHFB, respectively. In both cases, the strengths of the pairing force for neutrons (V_0^n) and protons (V_0^p) were adjusted either to the odd-even mass staggering or first (kinematic) moments of inertia (MoI) $\mathcal{J}^{(1)}$. Experimental and theoretical pairing gaps were estimated by using the three-point-mass-difference formula, which takes into account the influence of the deformation and blocking effects [40–42].

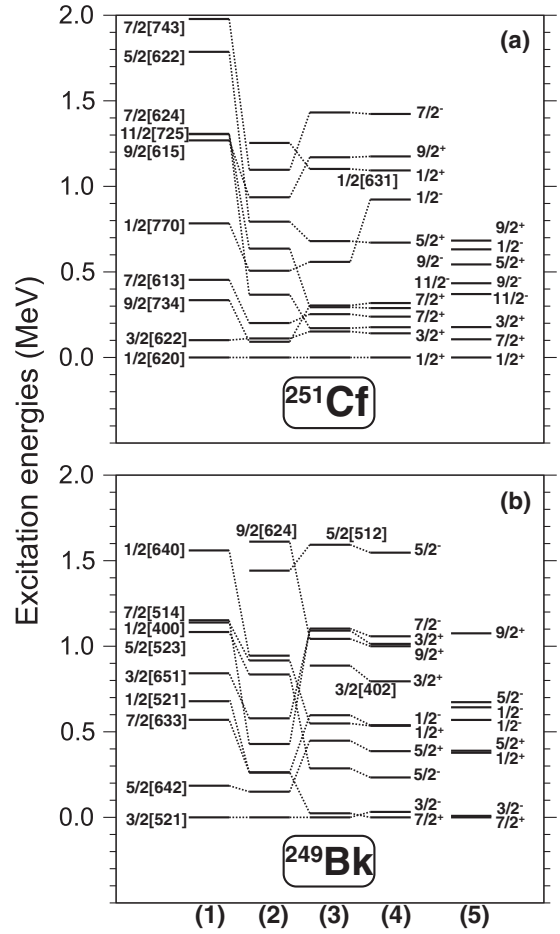

FIG. 1. The SHFB+LN excitation spectra of ^{251}Cf (top) and ^{249}Bk (bottom). Results obtained with the Skyrme EDFs SLy4 (1), UNEDF1 (2), UNEDF1$^{\rm SO}$ (3), and UNEDF1$^{\rm SO}_{\rm L}$ (4) are compared with experimental data (5) taken from the ENSDF database [43] and Refs [44,45].

Experimentally, the most detailed knowledge of the s.p. levels in the transuranium region comes from the energy spectra of ^{251}Cf and ^{249}Bk [5]. Therefore, the SHFB+LN blocking calculations were performed for these two nuclei and the excitation spectra obtained were compared with experimental data, see Fig. 1. In general, it is found that for SLy4 and UNEDF1, correct orbitals appear near the Fermi surface, however, the detailed agreement is not fully satisfactory. It should be noted that, with the most recent parametrization of Ref. [46], this situation does not improve. The most conspicuous differences between the data and calculations relate to positions of the intruder levels, which are highly dependent on the SO coupling constants $C_0^{\nabla J}$ and $C_1^{\nabla J}$ of the Skyrme EDFs. The possibility of reproducing the experimental spectra in odd-mass nuclei by changing the SO strengths was already discussed in Ref. [17].

In this work, focus was placed on the excitation energies of the $11/2^-$ state in ^{251}Cf with respect to the $1/2^+$ ground state and of the $3/2^-$ state in ^{249}Bk that is very close to the $7/2^+$ ground state. In theory, they correspond to the relative energies between the neutron ($11/2^-[725]$) and proton ($7/2^+[633]$) intruder levels, and the corresponding normal-parity states $1/2^+[620]$ and $3/2^-[521]$, respectively. The adjustment of parameters was performed by repeating the following two steps:

(i) By assuming a linear dependence of the neutron and proton excitation energies described above on the two coupling constants $C_0^{\nabla J}$ and $C_1^{\nabla J}$, the experimental and theoretical excitation energies of the $11/2^-$ state in ^{251}Cf and $3/2^-$ state in ^{249}Bk were matched.

(ii) By assuming a linear dependence of the neutron and proton mass staggering on the two pairing strengths, V_0^n and V_0^p, the experimental and theoretical values obtained from the mass tables of Ref. [47], that is, $\Delta_n^{(3)} = 532.1$ and $\Delta_p^{(3)} = 567.7$ keV, were matched.

In reality, it was found that the aforementioned dependencies were not strictly linear, and that the two steps were not really independent from one another, such that the procedure had to be repeated a few times, each time iterating toward the final desired values. For the SHFB+LN calculations the final values read

$$\left(C_0^{\nabla J}, C_1^{\nabla J}\right) = (-88.050, 8.458)\ \text{MeV fm}^5, \quad (1)$$

$$\left(V_0^n, V_0^p\right) = (-191.1, -235.3)\ \text{MeV}. \quad (2)$$

The SO coupling constants in Eq. (1) define the parameterization UNEDF1$^{\text{SO}}$. Since four theoretical parameters were adjusted to reproduce four experimental data points, no estimates of the error in the adjusted values are possible. However, the readjusted values (1) and (2) are still within 2–3 σ deviations from the UNEDF1 values (see the uncertainties σ that were estimated in Ref. [29]). In fact, it may very well be that a full readjustment of the UNEDF1 parameter set, performed with constraints on energy levels in the nobelium region, could result in a fit of a similar quality to that obtained for the original force.

Figure 2 (left panels) shows the dependence of the calculated SHFB+LN UNEDF1$^{\text{SO}}$ neutron and proton gaps on the pairing strengths V_0^n and V_0^p, respectively, with other parameters fixed at the values shown in Eqs. (1) and (2). Right panels show the analogous SHFB results.

With parametrization UNEDF1$^{\text{SO}}_{\text{L}}$ and pairing strengths of Eq. (2), cranking SHFB+LN and SHFB calculations for ^{246,248,250}Fm, ^{252,254}No, and ^{256}Rf were performed. In these nuclei, rotational bands have been measured experimentally. It was observed that, at lower frequencies, the calculations overestimate the measured kinematic MoI, $\mathcal{J}^{(1)}$, as shown in Fig. 3 for ^{252}No. The discrepancy is systematic and thus calls for a generic explanation, which most probably should be related to the overall strength of the pairing correlations. It means that, at the targeted level of precision, the pairing strengths inferred from the odd-even staggering and rotational properties are incompatible.

Therefore, in order to better compare relative values of the MoI in different nuclei, the pairing strengths $V_0^{n,p}$ of

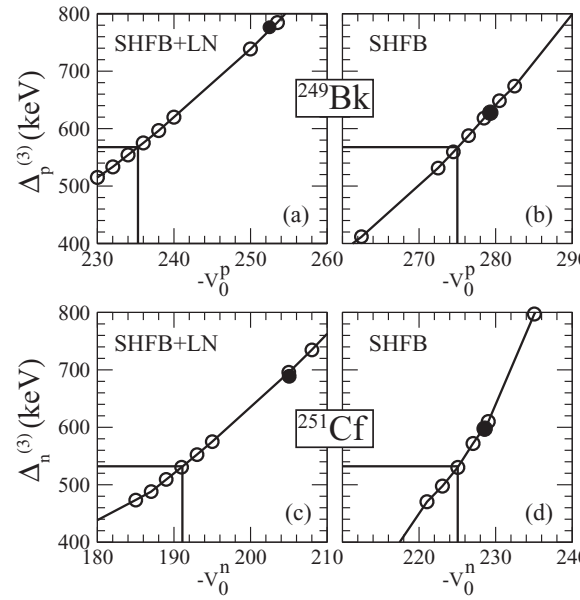

FIG. 2. The UNEDF1$^{\text{SO}}$ three-point mass differences $\Delta^{(3)}$ for protons in ^{249}Bk (top panels) and neutrons in ^{251}Cf (bottom panels) as functions of the proton and neutron pairing strengths, V_0^p and V_0^n, respectively. Left and right panels show the SHFB+LN and SHFB results, respectively. Vertical lines and full dots indicate values of the pairing strengths that give experimental values of $\Delta^{(3)}$ and $\mathcal{J}^{(1)}$, respectively.

Eq. (2) were scaled by a common factor f, so as to match the experimental value of $\mathcal{J}^{(1)}$ in ^{252}No at $\omega = 0.05$ MeV (see Fig. 3). Both for the SHFB+LN and SHFB calculations, the scaling gives values slightly larger than 1, namely $f = 1.073$ and 1.017, respectively, that is,

$$\left(V_0^n, V_0^p\right) = (-205.1, -252.5)\ \text{MeV, for SHFB + LN}, \quad (3)$$

$$\left(V_0^n, V_0^p\right) = (-228.6, -279.3)\ \text{MeV, for SHFB}. \quad (4)$$

This, in turn, leads to an increase of the calculated pairing gaps $\Delta_{n,p}^{(3)}$ by 150–200 keV, as shown by dots in Fig. 2. At this point, it is very difficult to say if the differences in pairing strengths, needed to describe the odd-even mass staggering in ^{251}Cf and ^{249}Bk, and the MoI in ^{252}No are significant. Both the gaps and the MoI are not only sensitive functions of pairing, but also

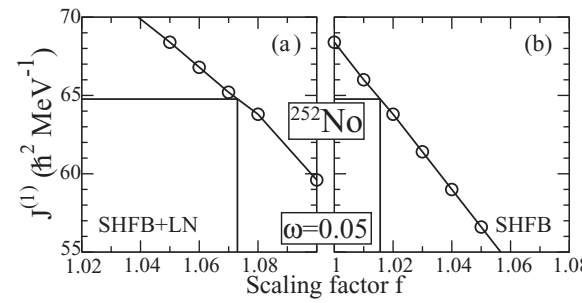

FIG. 3. Similar as in Fig. 2, but for the kinematic MoI $\mathcal{J}^{(1)}$, calculated in ^{252}No at the rotational frequency of $\omega = 0.05$ MeV, as functions of the pairing-strength scaling factors f; see text.

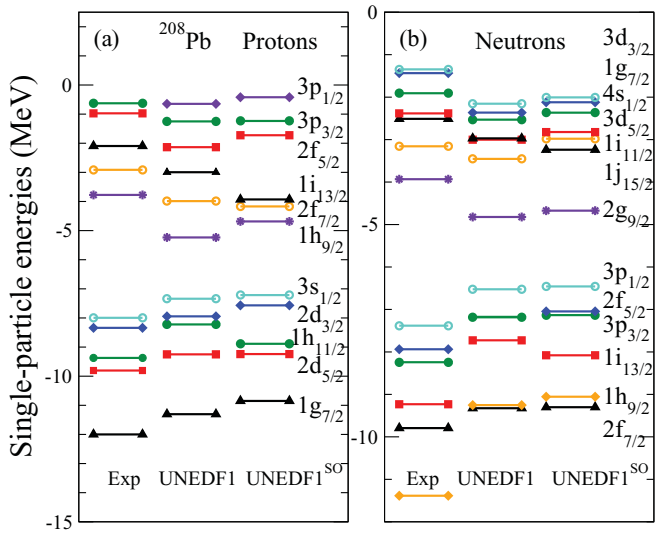

FIG. 4. (Color online) Proton (left) and neutron (right) s.p. spectra in ^{208}Pb, calculated for the UNEDF1 and UNEDF1^{SO} functionals and compared with evaluated experimental data [48].

depend on other fine details of the shell structure, which still can be imperfect, even after our careful adjustments of the SO strengths. Finally, for consistency, all results presented in this study were obtained with scaled pairing strengths of Eqs. (3) and (4). This includes all SHFB+LN excitation spectra shown in Fig. 1.

Tests performed for a larger HO basis of 969 states allow the precision of the results obtained to be estimated. Firstly, it is noted that the pairing properties do depend on the size of the HO space. For example, adjustments of the pairing strengths to odd-even mass staggering lead in the larger basis to values of V_0^n smaller by about 1% (SHFB+LN) or 5% (SHFB). At the same time, values of V_0^p are almost unaffected. This shows that values of the pairing strengths given in Eqs. (2)–(4) pertain to the specific size of the HO basis and cannot be considered as having any universal significance. However, when all adjustments of parameters are performed in the basis of 969 states, exactly in the same way they were performed for the 680 states, final values of MoI stay the same within 1 $\hbar^2$/MeV.

To further illustrate the degree of changes induced by modifying the SO and pairing parameters of the UNEDF1 functional, Figs. 4 and 5 show results obtained for the s.p. spectra in ^{208}Pb and fission barriers of ^{240}Pu, respectively. Here, identical numerical conditions and experimental data as those used in Ref. [29] are employed. It is seen that the ^{208}Pb s.p. energies obtained within the UNEDF1 and UNEDF1^{SO} functionals are very similar to one another, with slightly larger SO splittings of UNEDF1^{SO} being in somewhat better agreement with data. However, it should be noted that the overall discrepancies with respect to experimental data are significantly larger than the differences between them for both functionals.

For the ^{240}Pu fission barriers, the results depend significantly on the strength of the pairing correlations. Therefore,

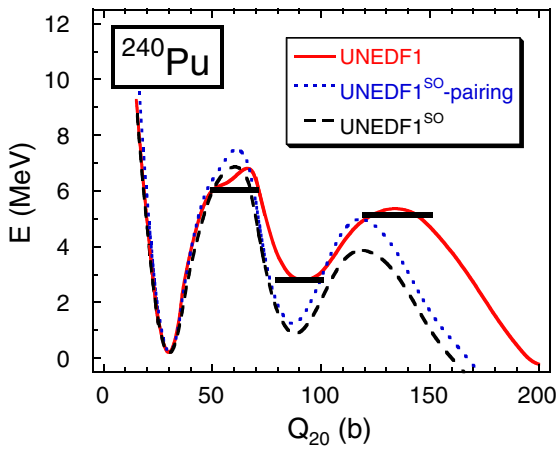

FIG. 5. (Color online) Fission barriers of ^{240}Pu, calculated for the UNEDF1 (solid line) and UNEDF1^{SO} (dashed line) functionals. The dotted line shows results for the hybrid functional using the UNEDF1^{SO} SO strengths and the original UNEDF1 pairing strengths. Horizontal lines illustrate the experimental energies as explained in Ref. [29].

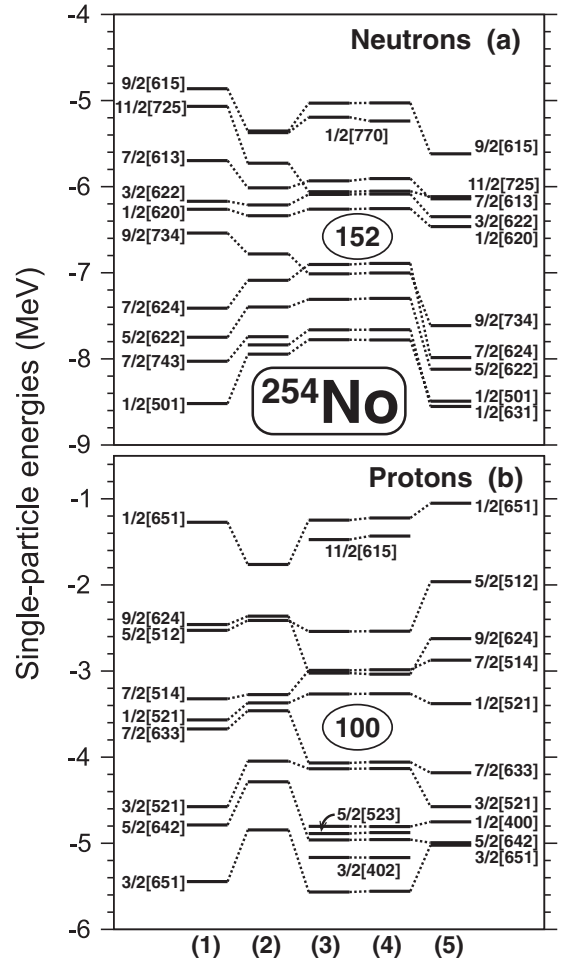

FIG. 6. Single-particle energies of neutrons (top) and protons (bottom) in ^{254}No. Columns (1)–(4) are labeled as in Fig. 1, whereas column (5) gives results calculated for the Woods-Saxon potential [51].

in Fig. 5 an additional dotted line shows the results obtained for the modified SO strengths of the UNEDF1^{SO} functional, but with the original UNEDF1 pairing strengths. It can be seen that at the top of barriers, the differences in pairing alone create significantly different energies. However, independently of the pairing strengths, the UNEDF1^{SO} excitation energies of the second minima turn out to be significantly underestimated. This shows that in a global fit of the UNEDF1^{SO} parameters, further readjustment of surface energy may still be required. At this point, it cannot be expected that after re-adjusting the spectroscopic SO properties, the detailed bulk nuclear energies should stay the same.

III. RESULTS

With the readjusted SO and pairing parameters, Eqs. (1) and (3), the UNEDF1^{SO} and UNEDF1$^{SO}_{L}$ excitation spectra of ^{251}Cf and ^{249}Bk agree quite well with the experimental data, see Fig. 1. The set UNEDF1$^{SO}_{L}$, based on the Landau parameters, gives energy levels that are only slightly different, by 100–200 keV, than those of the UNEDF1^{SO} set. The only exception is the $1/2^-[770]$ state in ^{251}Cf, which differs by about 400 keV.

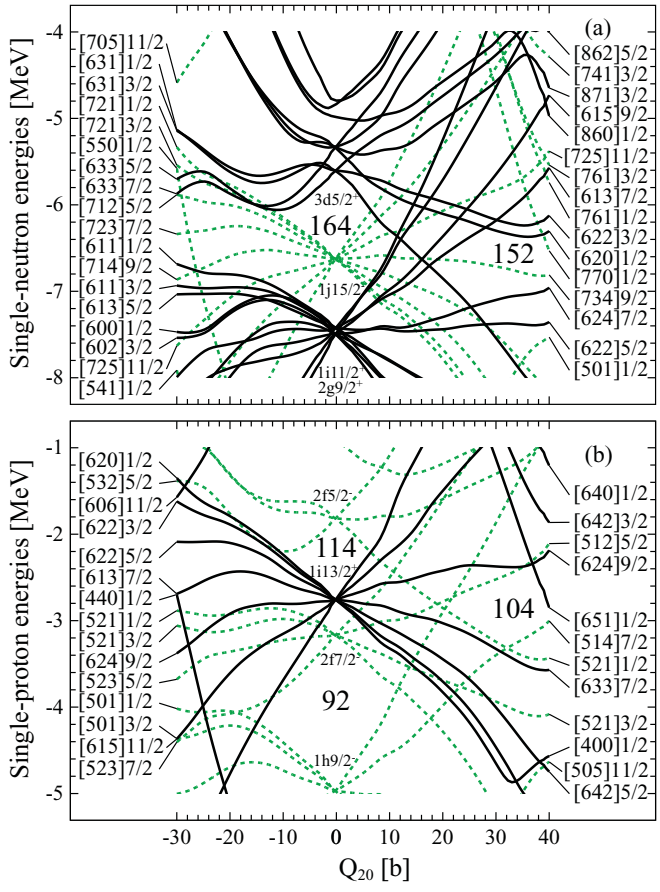

FIG. 7. (Color online) Neutron (top) and proton (bottom) Nilsson diagrams in ^{254}No calculated for the Skyrme EDF UNEDF1. Even- and odd-parity levels are drawn with solid and dashed lines, respectively.

For the neutron spectrum, the low-energy part is perfectly reproduced. The only more significant discrepancy between calculations and experiment is that there are two $7/2^+$ states obtained close to one another, whereas only one is seen in the data. The Nilsson numbers of these two states are $7/2^+[613]$ and $7/2^+[624]$, and they have particle and hole character, respectively. At higher energies, three levels, $5/2^+[622]$, $1/2^-[770]$, and $9/2^+[615]$, are more stretched compared to the experimental data, but their order is correctly reproduced.

Throughout the paper we use the standard concept of the Nilsson asymptotic quantum numbers [49,50], assigned to deformed s.p. states. Although these numbers are exact only in the limit of large deformations of the axial HO, based on determining the largest Nilsson components of deformed wave functions they are customarily assigned to all s.p. states. This creates a robust platform of describing various deformed configurations, which is most often valid across different models, and which is also routinely used in the discussions of experimental properties of deformed nuclei. This may create ambiguities only when more than one large Nilsson component is present in a given model wave function. In this context, we note that the Nilsson quantum numbers for $1/2^-$ state in our SHFB+LN calculation are $1/2^-[770]$, whereas in the analyses of experimental data [45], they are given as $1/2^-[750]$.

It is especially gratifying to see the proton $7/2^+[633]$ level almost degenerate with the $3/2^-[521]$. On the one hand, within

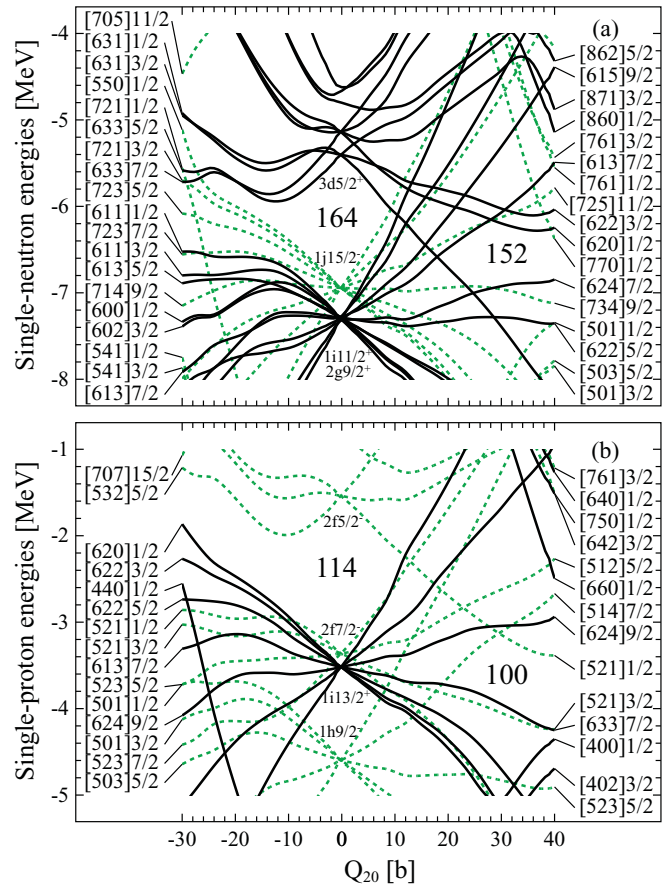

FIG. 8. (Color online) Same as in Fig. 7 but for the Skyrme EDF UNEDF1^{SO} derived in this work.

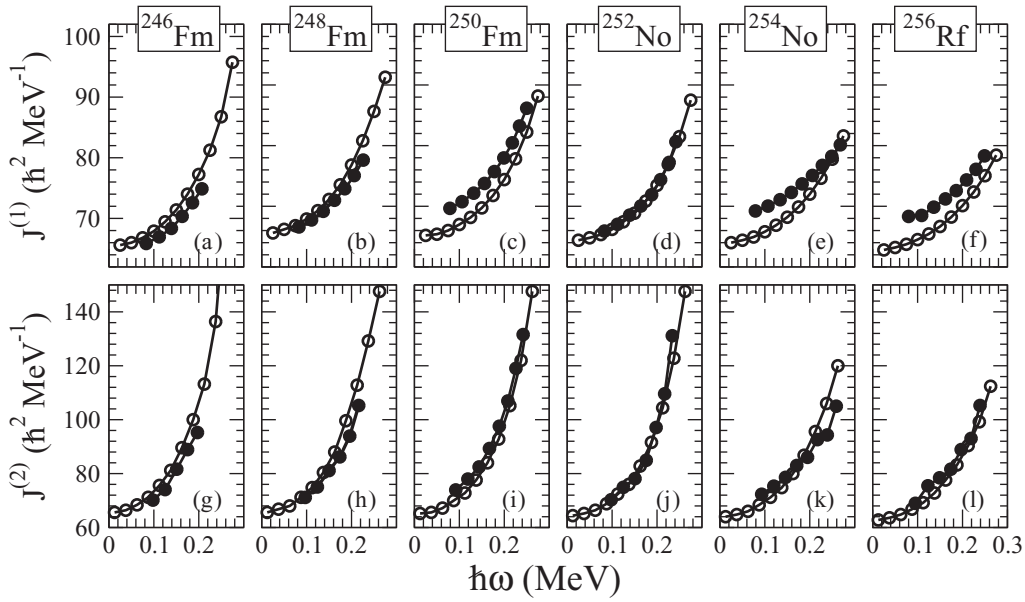

FIG. 9. The kinematic $\mathcal{J}^{(1)}$ (top) and dynamic $\mathcal{J}^{(2)}$ (bottom) MoI in ^{246}Fm, ^{248}Fm, ^{250}Fm, ^{252}No, ^{254}No, and ^{256}Rf as functions of the rotational frequency. Open circles show theoretical results whereas full dots denote experimental values.

the standard SO strengths, such a degeneracy is very difficult to obtain. On the other hand, in experiment it is a recurring feature of odd-proton nuclei in this region [52,53]. The rest of the low-energy spectrum is also in good agreement with experiment, with only the $5/2^-[523]$ state appearing lower in calculation than in experiment. This suggests that the proton $1h_{9/2^-}$ spherical shell may have been brought too close to the Fermi level. An additional $1/2^-[530]$ state seen in experiment is not present in the calculations [44].

The good agreement between the calculated and experimental spectra of odd-mass nuclei, prompted an analysis of the s.p. deformed shell structure resulting from the calculations. Although the deformed s.p. levels are not directly observable, they still nicely illustrate basic features of paired deformed systems. In Fig. 6, the s.p. levels of ^{254}No obtained for the EDF parametrizations that were shown in Fig. 1 are compared with those calculated for the Woods-Saxon potential [51] with deformation parameters taken from Ref. [8].

For the SLy4 EDF, the neutron and proton shell gaps open up at $N = 150$ and $Z = 98$ and 104, cf. Ref. [26]. The original UNEDF1 parametrization gives more compressed s.p. spectra, with no apparent neutron shell gap and the proton shell gaps also appearing at $Z = 98$ and 104. With the adjusted SO terms, the s.p. energies calculated with UNEDF1$^{\rm SO}$ show the shell gaps that open up at $N = 152$ and $Z = 100$. This result is very similar to the one obtained for the phenomenological Woods-Saxon potential, which in this region is considered to be consistent with experiment.

Figures 7 and 8 display for the UNEDF1 and UNEDF1$^{\rm SO}$ parametrizations, respectively, the s.p. energies as functions of the quadrupole moment (Nilsson diagrams). It is seen that the readjustment of the SO coupling constants results in the intruder neutron $1j_{15/2^-}$ and proton $1i_{13/2^+}$ spherical shells being shifted down by a few hundred keV with respect to the normal-parity levels. This, at deformation of $Q_{20} \approx 33$ b, opens up the deformed neutron $N = 152$ and proton $Z = 100$ gaps. At the same time it can be seen that the UNEDF1$^{\rm SO}$ parameters give the spherical proton-shell opening at $Z = 114$. It is noted that the issue of spherical shell gaps of superheavy nuclei, highly debated in the literature, in fact depends on a quite tiny readjustment of two poorly determined parameters of the underlying theory.

In Fig. 9, the calculated (cranked SHFB+LN with UNEDF1$^{\rm SO}_{\rm L}$) and experimental, kinematic ($\mathcal{J}^{(1)}$) and dynamic ($\mathcal{J}^{(2)}$) MoI are shown for six nuclei where experimental values are available. As discussed in Sec. II, increased pairing strengths (3), adjusted to the experimental value of the $\mathcal{J}^{(1)}$ MoI at $\omega = 0.05$ in ^{252}No are used. In the scale of Fig. 9, the agreement between the calculations and experiment is reasonably good. Especially the dynamic MoI $\mathcal{J}^{(2)}$ are reproduced almost perfectly. However, in this work focus is placed on the fine details of the rotational alignment, which may give hints concerning the underlying shell structure.

Therefore, in Fig. 10 an extended scale is used to compare the $\omega = 0.05$ MeV calculated and experimental values of $\mathcal{J}^{(1)}$. The latter were obtained by the standard Harris fits to experimental data [6]. Cranking calculations were performed for 18 even-even nuclei with $Z = 100$–104 and $N = 146$–156, with (SHFB+LN) and without (SHFB) the LN corrections. The SHFB+LN results show a rather smooth decrease of $\mathcal{J}^{(1)}$ with increasing neutron number, whereas those obtained for SHFB show at neutron number $N = 152$ pronounced peaks for No and Rf isotopes, or a kink for the Fm isotopes, giving a much better agreement with data. It is noted that similar trends were obtained with and without LN corrections, respectively, in Refs. [25] and [8]. These studies used different, relativistic and phenomenological, p-h mean-fields, but did not compare results obtained with and without LN corrections.

The appearance of a peak of $\mathcal{J}^{(1)}$ may indicate that the Fermi level reaches the s.p. shell gap. This results in a

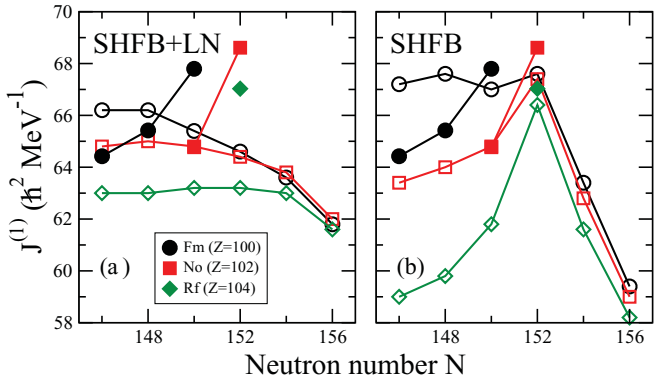

FIG. 10. (Color online) The kinematic MoI $\mathcal{J}^{(1)}$ of the Fm, No, and Rf isotopes calculated at the rotational frequency of $\omega = 0.05$ MeV. Left and right panels show the SHFB+LN and SHFB results. Open and full symbols show theoretical results and available experimental data, respectively.

quenching of pairing correlations, and thus in an increase of the MoI. The LN correlation, as in any other method to restore the particle-number symmetry, tends to enhance pairing effects, even at shell gaps. Therefore, such methods lead to smoother dependencies of pairing on particle numbers and thus wash out sudden changes in the MoI. It seems that this mechanism leads, at variance with experiment, to a complete disappearance of the effects of the $N = 152$ shell gap on rotational properties.

IV. CONCLUSION

In the present work, the rotational properties of very heavy nuclei have been investigated through the magnifying glass of a spectroscopic-quality energy density functional, which was specifically adjusted to this region of nuclei. This approach is complementary to numerous studies performed using globally adjusted functionals, where gross features are usually nicely reproduced, but finer details, which are of great interest to experimentalists, are often not.

Indeed, by adjusting the SO coupling constants and pairing strengths to odd-even mass staggering and intruder excitation energies in ^{251}Cf and ^{249}Bk, it has been possible to obtain good agreement with data. Moreover, the obtained deformed shell structure then revealed pronounced shell gaps, which opened up at $Z = 100$ and $N = 152$, again in agreement with general features of the experimental data in this region of nuclei. Cranking calculations performed with the modified parameters also gave a fair agreement with experiment. However, under detailed comparison at a much finer level than usually performed, the following deficiencies of the description were revealed:

(i) The pairing strengths needed for the precise description of the odd-even mass staggering and those needed for a precise description of the moments of inertia are not exactly the same.

(ii) The approximate particle-number projection, performed using the Lipkin-Nogami method, gives a dependence of moments of inertia on particle numbers which is too smooth. It seems that the particle-number restoration washes out the deformed shell gaps, which is not compatible with data. This is puzzling, as in principle the particle-number conserving approach should give a superior description of the experimental data.

It is suggested that, within the current restricted parametrizations of the energy density functionals, further global improvement of precision in reproducing experimental data is unlikely. Of course, much more work is needed before extended parametrizations can be implemented and tested. In the mean time, local focused adjustments, like the one performed in this study, can give hints as to which elements of the description need more attention than others. It is hoped that the two deficiencies identified in this work may help in the future quest for precision.

ACKNOWLEDGMENTS

This work was supported in part by the Academy of Finland and University of Jyväskylä within the FIDIPRO program, the Centre of Excellence Programme 2012–2017 (Nuclear and Accelerator Based Physics Programme at JYFL), the European Research Council through the SHESTRUCT project (Grant Agreement No. 203481), the Office of Nuclear Physics, U.S. Department of Energy (DOE) under Contracts No. DE-FG02-96ER40963 (University of Tennessee) and No. DE-SC0008499 (NUCLEI SciDAC Collaboration), and the Polish National Science Center under Contract No. 2012/07/B/ST2/03907. The CSC-IT Center for Science Ltd, Finland, is acknowledged for the allocation of computational resources.

[1] D. Rudolph *et al.*, Phys. Rev. Lett. **111**, 112502 (2013).
[2] S. Hofmann and G. Münzenberg, Rev. Mod. Phys. **72**, 733 (2000).
[3] Y. T. Oganessian, J. Phys. G **34**, R165 (2007).
[4] S. Hofmann, Radiochim. Acta **99**, 405 (2011).
[5] R.-D. Herzberg and P. T. Greenlees, Prog. Part. Nucl. Phys. **61**, 674 (2008).
[6] P. T. Greenlees *et al.*, Phys. Rev. Lett. **109**, 012501 (2012).
[7] S. Nilsson, J. Nix, A. Sobiczewski, Z. Szymaski, S. Wycech, C. Gustafson, and P. Mller, Nucl. Phys. A **115**, 545 (1968).
[8] A. Sobiczewski, I. Muntian, and Z. Patyk, Phys. Rev. C **63**, 034306 (2001).
[9] A. Sobiczewski and K. Pomorski, Prog. Part. Nucl. Phys. **58**, 292 (2007).
[10] A. Sobiczewski, Radiochim. Acta **99**, 395 (2011).
[11] H. L. Liu, F. R. Xu, and P. M. Walker, Phys. Rev. C **86**, 011301 (2012).
[12] Z.-H. Zhang, J. Meng, E.-G. Zhao, and S.-G. Zhou, Phys. Rev. C **87**, 054308 (2013).
[13] M. Bender, P.-H. Heenen, and P.-G. Reinhard, Rev. Mod. Phys. **75**, 121 (2003).

[14] S. Ćwiok, J. Dobaczewski, P.-H. Heenen, P. Magierski, and W. Nazarewicz, Nucl. Phys. A **611**, 211 (1996).
[15] S. Ćwiok, W. Nazarewicz, and P. H. Heenen, Phys. Rev. Lett. **83**, 1108 (1999).
[16] T. Duguet, P. Bonche, and P.-H. Heenen, Nucl. Phys. A **679**, 427 (2001).
[17] M. Bender, P. Bonche, T. Duguet, and P.-H. Heenen, Nucl. Phys. A **723**, 354 (2003).
[18] J. L. Egido and L. M. Robledo, Phys. Rev. Lett. **85**, 1198 (2000).
[19] J.-P. Delaroche, M. Girod, H. Goutte, and J. Libert, Nucl. Phys. A **771**, 103 (2006).
[20] M. Warda and J. L. Egido, Phys. Rev. C **86**, 014322 (2012).
[21] A. V. Afanasjev, T. L. Khoo, S. Frauendorf, G. A. Lalazissis, and I. Ahmad, Phys. Rev. C **67**, 024309 (2003).
[22] D. Vretenar, A. V. Afanasjev, G. Lalazissis, and P. Ring, Phys. Rep. **409**, 101 (2005).
[23] E. Litvinova, Phys. Rev. C **85**, 021303 (2012).
[24] V. Prassa, T. Nikšić, G. A. Lalazissis, and D. Vretenar, Phys. Rev. C **86**, 024317 (2012).
[25] A. V. Afanasjev and O. Abdurazakov, Phys. Rev. C **88**, 014320 (2013).
[26] M. Bender and P.-H. Heenen, J. Phys.: Conf. Ser. **420**, 012002 (2013).
[27] P. Klüpfel, P.-G. Reinhard, T. J. Bürvenich, and J. A. Maruhn, Phys. Rev. C **79**, 034310 (2009).
[28] M. Kortelainen, T. Lesinski, J. Moré, W. Nazarewicz, J. Sarich, N. Schunck, M. V. Stoitsov, and S. Wild, Phys. Rev. C **82**, 024313 (2010).
[29] M. Kortelainen, J. McDonnell, W. Nazarewicz, P.-G. Reinhard, J. Sarich, N. Schunck, M. V. Stoitsov, and S. M. Wild, Phys. Rev. C **85**, 024304 (2012).
[30] M. Kortelainen, J. Dobaczewski, K. Mizuyama, and J. Toivanen, Phys. Rev. C **77**, 064307 (2008).
[31] M. Kortelainen, J. McDonnell, W. Nazarewicz, E. Olsen, P.-G. Reinhard, J. Sarich, N. Schunck, S. Wild, D. Davesne, J. Erler, and A. Pastore, arXiv:1312.1746.
[32] M. Zalewski, J. Dobaczewski, W. Satuła, and T. R. Werner, Phys. Rev. C **77**, 024316 (2008).
[33] N. Schunck, J. Dobaczewski, J. McDonnell, W. Satuła, J. Sheikh, A. Staszczak, M. Stoitsov, and P. Toivanen, Comput. Phys. Commun. **183**, 166 (2012).
[34] N. Schunck *et al*. (unpublished).
[35] N. Schunck, J. Dobaczewski, J. McDonnell, J. Moré, W. Nazarewicz, J. Sarich, and M. V. Stoitsov, Phys. Rev. C **81**, 024316 (2010).
[36] E. Chabanat, P. Bonche, P. Haensel, J. Meyer, and R. Schaeffer, Nucl. Phys. A **635**, 231 (1998).
[37] M. Bender, J. Dobaczewski, J. Engel, and W. Nazarewicz, Phys. Rev. C **65**, 054322 (2002).
[38] J. Dobaczewski, W. Nazarewicz, and M. V. Stoitsov, Eur. Phys. J. A **15**, 21 (2002).
[39] M. V. Stoitsov, J. Dobaczewski, W. Nazarewicz, S. Pittel, and D. J. Dean, Phys. Rev. C **68**, 054312 (2003).
[40] W. Satuła, J. Dobaczewski, and W. Nazarewicz, Phys. Rev. Lett. **81**, 3599 (1998).
[41] F. R. Xu, R. Wyss, and P. M. Walker, Phys. Rev. C **60**, 051301 (1999).
[42] J. Dobaczewski, P. Magierski, W. Nazarewicz, W. Satuła, and Z. Szymański, Phys. Rev. C **63**, 024308 (2001).
[43] Evaluated Nuclear Structure Data File, http://www.nndc.bnl.gov/ensdf/.
[44] I. Ahmad, F. G. Kondev, E. F. Moore, M. P. Carpenter, R. R. Chasman, J. P. Greene, R. V. F. Janssens, T. Lauritsen, C. J. Lister, D. Seweryniak, R. W. Hoff, J. E. Evans, R. W. Lougheed, C. E. Porter, and L. K. Felker, Phys. Rev. C **71**, 054305 (2005).
[45] I. Ahmad, J. P. Greene, E. F. Moore, F. G. Kondev, R. R. Chasman, C. E. Porter, and L. K. Felker, Phys. Rev. C **72**, 054308 (2005).
[46] K. Washiyama, K. Bennaceur, B. Avez, M. Bender, P.-H. Heenen, and V. Hellemans, Phys. Rev. C **86**, 054309 (2012).
[47] G. Audi, A. H. Wapstra, and C. Thibault, Nucl. Phys. A **729**, 337 (2003).
[48] N. Schwierz, I. Wiedenhover, and A. Volya, arXiv:0709.3525.
[49] S. Nilsson, Mat. Fys. Medd. Dan. Vid. Selsk. **29**, No. 16, 1 (1955).
[50] P. Ring and P. Schuck, *The Nuclear Many-Body Problem* (Springer, Berlin, 1980).
[51] S. Cwiok, J. Dudek, W. Nazarewicz, J. Skalski, and T. Werner, Comput. Phys. Commun. **46**, 379 (1987).
[52] F. P. Heßberger, S. Antalic, B. Streicher, S. Hofmann, D. Ackermann, B. Kindler, I. Kojouharov, P. Kuusiniemi, M. Leino, B. Lommel, R. Mann, K. Nishio, S. Saro, and B. Sulignano, Eur. Phys. J. A **26**, 233 (2005).
[53] Y. Shi, J. Dobaczewski, P. T. Greenlees, J. Toivanen, and P. Toivanen, in *Proceedings of the Fifth International Conference on Fission and Properties of Neutron-Rich Nuclei*, edited by J. H. Hamilton and A. V. Ramayya (World Scientific, New Jersey, 2014), p. 381; Y. Shi, J. Dobaczewski, P. T. Greenlees, J. Toivanen, and P. Toivanen, arXiv:1303.0197.